Drug Design, Development and Therapy

Dovepress
open access to scientific and medical research

Open Access Full Text Article

ORIGINAL RESEARCH

Enhancing Betulinic Acid Dissolution Rate and Improving Antitumor Activity via Nanosuspension Constructed by Anti-Solvent Technique

This article was published in the following Dove Press journal:
Drug Design, Development and Therapy

Shuqi Li[1–3]
Jie Zhang[1–3]
Yuqi Fang[1–3]
Jun Yi[1]
Zhufen Lu[2,3]
Yanzhong Chen[2,3]
Bohong Guo[1–3]

[1]Department of Pharmaceutics, School of Pharmacy, Guangdong Pharmaceutical University, Guangzhou, People's Republic of China; [2]Guangdong Provincial Key Laboratory of Advanced Drug Delivery Systems, Guangdong Pharmaceutical University, Guangzhou, People's Republic of China; [3]R&D Team for Formulation Innovation, Guangdong Pharmaceutical University, Guangzhou, People's Republic of China

Purpose: The aim of this study was to prepare and evaluate betulinic acid nanosuspension (BA-NS) for new drug delivery to enhance its solubility and in vitro anti-tumor activity.

Methods: BA-NS was formulated by an anti-solvent precipitation method using the Box-Behnken design (BBD). Particle size (PS) and Zeta potential were measured by laser particle size analysis. The drug solid state after freeze drying was characterized by scanning electron microscope (SEM), transmission electron microscope (TEM), differential scanning calorimetry (DSC), X-ray powder diffraction (XRPD) and Fourier transform infrared spectroscopy (FTIR) after freeze drying. The saturation solubility and dissolution rate were determined by solubility assay and in vitro dissolution studies, respectively. The in vitro cytotoxicity assay was performed using 3-(4,5-dimethylthiazole)-2,5-diphenltetraazolium bromide (MTT) method.

Results: The PS was 129.7±12.2 nm having a Zeta potential of −28.1±4.5 mV and the polydispersity index (PDI) was 0.231±0.013, which confirmed that the nanosuspension was in the stable amorphous state. A series of characterization experiments demonstrated that nanoparticles retained original effective structure and existed as spherical or near-spherical nanoparticles in the nanosuspension, but the drug transferred from the crystal state to the amorphous state. The form of lyophilized BA-NS was very successful in enhancing the dissolution rate in PH-dependent way. The cytotoxicity assay revealed that BA-NS could significantly enhance the in vitro anti-proliferation against tumor cells compared to the BA suspension (BA-S).

Conclusion: The BA-NS can remarkably improve solubility and in vitro antitumor activity, which seems very promising for the treatment of cancers in practical application.

Keywords: betulinic acid, nanosuspension, anti-solvent precipitation, Box-Behnken design, cytotoxicity

Correspondence: Yanzhong Chen
Guangdong Provincial Key Laboratory of Advanced Drug Delivery Systems, Guangdong Pharmaceutical University, Guangzhou 510006, People's Republic of China
Tel +86 20 3935 2678
Fax +86 20 3935 2501
Email doctor.c@163.com

Bohong Guo
Department of Pharmaceutics, School of Pharmacy, Guangdong Pharmaceutical University, 280 East Waihuan Road, Guangzhou Higher Education Mega Center, Guangzhou 510006, People's Republic of China
Tel +86 20 3935 2117
Fax +86 20 3935 2129
Email guobohong@gdpu.edu.cn

Introduction

Betulinic acid (3β-hydroxy-lup-20(29)-en-28-oic acid) (BA) as shown in Figure 1 is a triterpene of natural origin isolated from various plants and is widely distributed in the plant kingdom.[1] BA plays a crucial role as a resource for potential anticancer compounds for its certain advantages in abundant supply from common natural sources, such as inexpensive and available.[2] Previous studies have potently illustrated BA exhibited a variety of biological activities including the prevention and treatment of human immunodeficiency virus (HIV) infection, anti-tumor, antibacterial, antimalarial, anti-inflammatory, anthelmintic and antioxidant activities.[3–5]

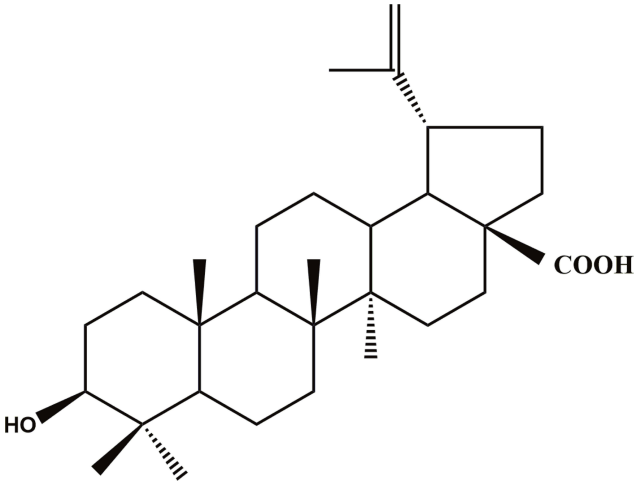

Figure 1 Chemical structure of BA.
Abbreviation: BA, betulinic acid.

Particularly, BA performs significant anti-tumor activity in melanoma cell lines.[6] BA can inhibit the broad spectrum of tumor cell line proliferation, such as prostate, neuroblastoma, melanoma, colon, breast and lung cells.[7–10] In fact, BA is a poorly water-soluble compound, and difficult to develop as a drug product. Moreover, BA has many problems in clinical use, such as poor aqueous solubility, short blood circulation time, lack of targeting and certain severe toxic side effects.[11] Recent studies indicate new drug delivery systems would avoid these drawbacks.[12–14] In the current study, we reported the preparation of BA-NS using the anti-solvent method, characterization of the nanoparticles and in vitro cell cytotoxicity on HeLa, A549 and HepG2 by MTT method.

Nanosuspension (100–1000 nm) technology is defined as an approach that a small amount of surfactants, polymeric materials or a mixture of both for stabilization become a universal formulation to process poorly soluble drugs with low solubility on account of enlarging surface area and decreasing particle diameter.[15] The reduction in the drug particle size to the nanometer range enhances its solubility as well as dissolution rate, which are both essential parameters for improving the bioavailability of drugs and convenience in clinical utilization.[16,17] Nanosuspension, a promising drug delivery system, has plenty of advantages, including the reduced systemic toxicity of drug, the enhanced stability and duration of drug action and the improved pharmacodynamic action.[18] Nanotechnology also can be used to prepare CaO_2 nanocrystals for increasing antibacterial effect.[19]

The preparation methods of nanosuspension can be grouped into two principal categories: "Top-down technology" and "Bottom-up technology." The top-down technologies are disintegration methods, and basically depend on mechanical wear to shatter large crystalline particles into smaller nanoparticles, comprising media milling, microfluidization and high-pressure homogenization. The bottom-up methods are described as progresses of controlled precipitation and crystallization, which means dissolving the drug in a solvent and precipitating it under a controlled manner to nanoparticles, including anti-solvent method, supercritical fluid process, spray drying and emulsion-solvent evaporation.[20,21] In contrast to the top-down methods, the bottom-up methods have many obvious advantages, such as simple setup, smaller particle size by lower energy and simple laboratory apparatus.[22] Antisolvent precipitation technology is a promising technique to prepare nano-sized drug particles, which exerts some superiorities, including straightforward, rapid and easy to perform.[23]

Materials and Methods

Material

BA (purity ≥98%) was obtained from Nanjing Zelang Medical Technology Co., Ltd. (Nanjing, China). Sodium dodecyl sulfate (SDS) was purchased from Fengli Jingqiu Pharmaceutical Co., Ltd. (Beijing, China), and polyvinylpyrrolidone (PVP) K29-32 was kindly provided by ASHLAND (The United States). Acetonitrile and methanol (HPLC grade reagent) were obtained from Merck Inc. (Darmstadt, Germany). Dulbecco's modified Eagle's medium (DMEM), fetal bovine serum (FBS) and dimethyl sulfoxide (DMSO) were supplied by Sigma-Aldrich (St. Louis, MO, USA). HeLa cells (human cervical adenocarcinoma), A549 cells (human lung adenocarcinoma) and HepG2 (human hepatocellular carcinoma) were purchased by the American Type Culture Collection (ATCC) (Manassas, VA, USA)

Preparation of BA-NS

The anti-solvent precipitation method was employed to prepare BA-NS. The operating conditions and stabilizers were selected based on our multiple prescription screening in anti-solvent precipitation method of BA. As shown in Figure 2, BA was first dissolved in moderate ethanol at room temperature to form the organic phase and then filtrated through a 0.45-μm millipore syringe filter to remove any solid impurities. Meanwhile, polyvinyl

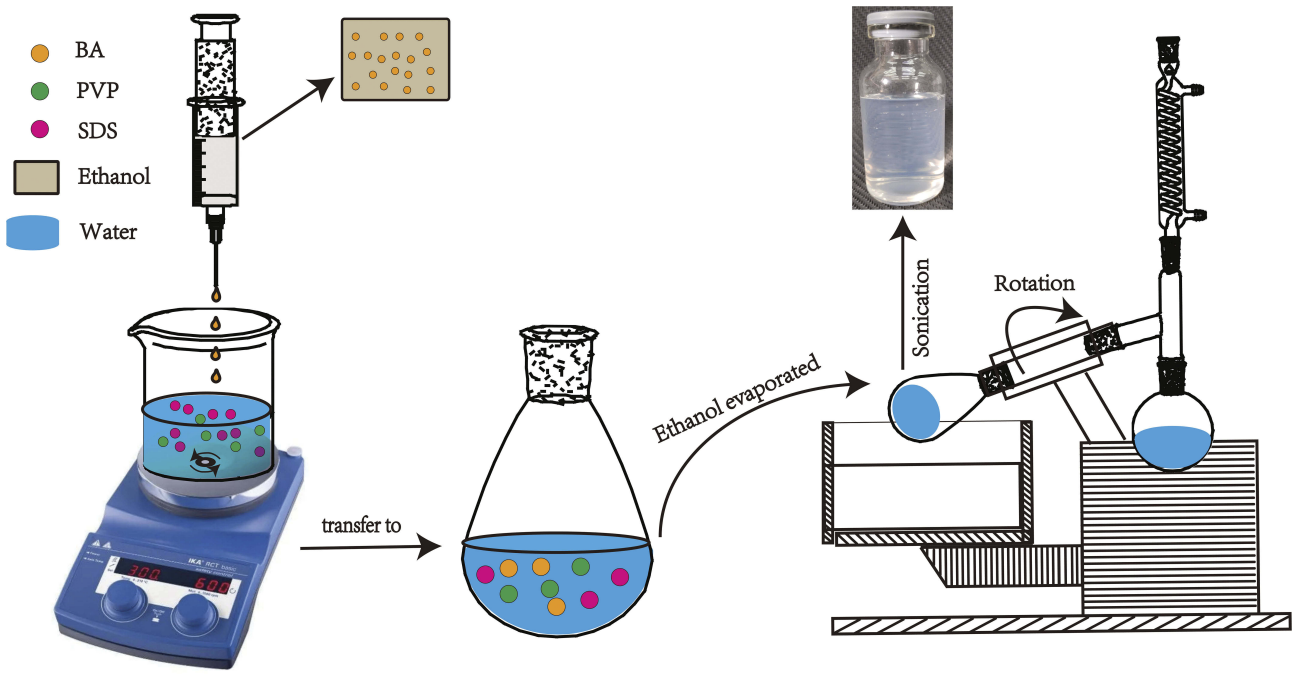

Figure 2 Schematic illustration of the formation of BA-NS.
Abbreviations: BA, betulinic acid; PVP, polyvinylpyrrolidone; SDS, sodium dodecyl sulfate; BA-NS, betulinic acid nanosuspension.

pyrrolidone (PVP) K29-32 and sodium dodecyl sulfate (SDS) were selected as optimum stabilizers and dispersed in distilled water. 12 mL of organic solution was gently added dropwise into 15 mL of anti-solvent with a magnetic stirring apparatus under stirring condition for 10 min. Afterward, the above suspension was kept under vacuum at 45°C to remove the ethanol. To obtain a homogeneous size, the nanosuspension was sonicated (Scientz-IID Ultrasonic Cell Disruptor; Ningbo Scientz Biotechnology Co., Ltd, Ningbo, China) at 380 W of 2 s after every 2 s interval for a total time of 5 min. All the resultant suspension was centrifuged for 10 min at 10,000 rpm using a refrigerated centrifuge at 4°C to remove free BA. For the long-term stability of the product and subsequent characterization analysis, the freshly prepared nanosuspension was lyophilized into dry powders using a freeze dryer (LGJ-150; Beijing Sihuan, China) and stored in the drying oven.

HPLC Analysis

The quantitative analysis of BA was analyzed by high-performance liquid chromatography (HPLC) using an Agilent 1200 system (Sunnyvale, USA) with a reverse phase C18 column (5 μm, 4.6 × 250 mm, DIKMA Diamonsil) at room temperature. The mobile phase composed of a mixture of acetonitrile and purified water (80:20, v/v), and adjusted with acetic acid to pH 3. The mobile phase was filtered through a 0.45-μm microporous membrane and degassed ultrasonically prior to use. Standard solutions of BA were prepared by diluting the appropriate volume of stock solution in methanol and filtering with 0.22-μm microporous membranes. The injection volume was 20 μL, the detector was set at 210 nm and the flow rate was set at 1.0 $mL \cdot min^{-1}$.

Particle Size and Zeta Potential

The determination of the PS and the PDI of the nanosuspension was performed by dynamic light scattering (DLS), using a laser-scattered particle analyzer (Beckman Coulter Instruments, Fullerton, CA, USA). Zeta potential was measured by Nano Particle Analyzer (Beckman Coulter Instruments). The samples were determined in triplicate at room temperature.

TEM

The morphological evaluation of BA-NS was performed with a Hitachi-7650 (Hitachi Co., Ltd., Tokyo, Japan). Briefly, the sample was adsorbed onto the copper grid and air-dried at room temperature and was negatively stained using a 1% (w/v) uranyl acetate solution for 30 s before the TEM analysis.

SEM

BA and the nanosuspension were examined by SEM to visualize the surface morphology. Samples were coated with a sputter coater on aluminum under an argon atmosphere in a high vacuum evaporator using a gold sputter module with the electrical potential of 2.0 kV at 30 mA for 240 s. The coated samples were scanned and photographs were imagined by SEM (LEO 1430VP, Germany) at various magnifications.

DSC Analysis

The DSC (DSC 8500; Perkin Elmer, San Jose, California, USA) measurements were analyzed in a temperature range of 30–350°C at a heating rate of 10°C/min in nitrogen gas. Accurately weighed 6-mg samples (BA, BA-NS, physical mixture) were placed in a sealed aluminum pan and the melting point and heat of fusion were measured using the DSC software.

XRPD Detection

The XRD pattern of samples was recorded using X-ray diffractometer (Empyrean, Netherlands) by exposing them to Cu Kα as the source of radiation. All samples were scanned from 3° to 55° with a tube voltage of 40 kV and a tube current of 40 mA, a step size of 0.04° and a step time of 40 s. Samples investigated using XRPD analysis were the same as those of DSC analysis.

FTIR Spectroscopy

The spectra of BA powders, physical mixture and nanosuspension were collected using Spectrum 100 (Perkin Elmer, San Jose, California, United States) infrared spectrophotometer. Samples were prepared in KBr disc (1-mg sample/100 mg KBr) with a hydrostatic pressure at a force of 40 psi for 4 min. The scanning was performed in the range of 500–4000 cm^{-1}.

Solubility

Excessive freeze-dried BA-NS powders were dissolved in 50 mL of deionized water in a supersaturated state. Afterward, the solution was shaken in a constant-temperature shaker (WTS-031; Honglang, China) at 37°C for 48 h. The final suspension was centrifuged at 10,000 $r{\cdot}min^{-1}$ for 10 mins and filtered using a 0.22-μm micropore film. The peak area of BA was determined by HPLC. Each sample was analyzed in triplicate.

Dissolution Rate

In vitro dissolution studies (BA, physical mixture and lyophilized nanosuspension) were performed using a dissolution apparatus (ZRS-8G, Tianjin Tianda Technology Co., Ltd., China) according to the FDA paddle method in phosphate-buffered saline (PBS) solutions at pH 1.2, 4.8 and 7.4. 2.5 mL of aliquots were removed and replaced with the same volume of the dissolution media at a regular time interval. The BA content of the supernatant was filtered using a 0.22-μm micropore film and analyzed by the HPLC method. All the samples were carried out in triplicate.

Design of Experiments

In our experiment, in order to develop and optimize the formulation of BA-NS, the three-factor and three-level Box–Behnken experimental design (BBD) were determined based on the results of the preliminary experiments.[24]

The three independent variables in Table 1 were assigned as X_1 (concentration of BA), X_2 (concentration of PVP) and X_3 (concentration of SDS) and were arranged into three grades, including high value (+1), intermediate value (0) and low value (−1). While PS and PDI (Y_1 and Y_2) were defined as dependent variables. The correlation between a dependent variable (Y) and an independent variable (X) was evaluated by a second-order polynomial equation. Table 2 lists 17 experiments and 5 centre points.[25] The optimal combination of variable levels was determined through multi-response optimization techniques and based on the experimental results. The multiple factors linear and binomial fitting were applied to each factor using Design Expert 8.0.6 software. And the corresponding polynomial equation was as follows.[26]

$$Y = \beta_0+\beta_1X_1+\beta_2X_2+\beta_3X_3+\beta_4X_1X_2+\beta_5X_1X_3 +\beta_6X_2X_3+\beta_7X_1^2+\beta_8X_2^2+\beta_9X_3^2$$

where Y is the target of the optimized response, β_0 is the intercept coefficient, representing the arithmetic mean of all quantitative results of 17 random experiments, β_1–β_9 are the interaction and quadratic coefficients from the

Table 1 Variables and Levels in the BBD

Independent Variables	Levels		
	−1	0	1
Concentration of BA ($mg{\cdot}mL^{-1}$)	0.8	1	1.2
Concentration of PVP ($mg{\cdot}mL^{-1}$)	0.5	1	1.5
Concentration of SDS ($mg{\cdot}mL^{-1}$)	2	3	4

Abbreviation: BBD, Box–Behnken experimental design.

Table 2 Design and Results of BBD

Run	Input Variables			Output Variables	
	X_1	X_2	X_3	PS (nm)	PDI
1	1	1	0	450.6	0.297
2	−1	0	1	679.2	0.489
3	0	1	1	456	0.273
4	0	1	−1	148.1	0.161
5	0	0	0	360.4	0.265
6	0	0	0	189.7	0.177
7	0	−1	1	498.5	0.395
8	0	0	0	203.5	0.128
9	1	0	1	132.6	0.275
10	0	0	0	215.8	0.121
11	1	0	−1	276.9	0.191
12	0	−1	−1	246	0.178
13	−1	1	0	675.1	0.203
14	−1	−1	0	767.3	0.408
15	0	0	0	248.6	0.128
16	−1	0	−1	220.9	0.137
17	1	−1	0	300.5	0.149

Abbreviations: BBD, Box–Behnken experimental design; PS, particle size; PDI, polydispersity index.

values of Y, X_1, X_2 and X_3 are the independent factors, X_1^2, X_2^2 and X_3^2 are quadratic terms.

Stability Studies

The stability of the BA-NS was investigated after storage for 30 days at 4°C. The PS and PDI on days 0 and 30 were measured by a laser-scattered particle analyzer, and then the appearances of BA-NS were observed.

Cell Cultures: HeLa, A549 and HepG2 Cell Lines

HeLa, A549 and HepG2 were cultured under standard cell culture conditions (37°C in an atmosphere with $CuSO_4$ of 5% CO_2) in DMEM medium supplemented with 10% (v/v) heat-inactivated FBS, 1% penicillin (200 U/mL) and streptomycin (100 μg/mL). Cells were served on 25-cm^2 culture flasks or in various plates and used for seeding and then treated after getting 80–90% confluency.

Preparation of BA-S

A CMC-Na aqueous solution (1%, w/v) was selected as the suspending agent. BA was added to the suspending agent and dispersed uniformly with water bath sonication. The final concentration of the BA-S was set as 1 mg/mL.

Cytotoxic Activity Evaluation in vitro

The use of the yellow tetrazolium salt has increased as an indicator of cytotoxic activity evaluation in vitro of BA-S and BA-NS treated with tumor cells. For the MTT assay, 100 μL of suspension was added into 96-well microplates (1×10^4 cells/well) and incubated at 37°C, 5% CO_2 for overnight. The cells treated with different concentrations of BA-S or BA-NS (5–70 μM), and blank-NS was added equivalent volume to BA-NS into microplates with cell culture medium, the cells were continuously exposed to the drugs for 48 h with DMEM+10%FBS. Subsequently, adding 10 μL of MTT (5 mg/mL) and 90 μL DMEM without serum per well, and the plate was incubated for another 4h, then the above suspension was removed and replaced with 100 μL of DMSO to dissolve the formazan crystal by shaking for 10 min. The absorbance was measured by a Microplate Reader at 490 nm, and the experiments were determined in triplicate. The survival rate of cells was measured as follows:[27]

$$\text{Cell viability}(\%) = \frac{\text{Absorbance}_{\text{sample}}}{\text{Absorbance}_{\text{control}}} \times 100\%$$

Statistical Analysis

All data were expressed as mean ± standard deviation (SD) using SPSS Version 20.0 software (SPSS, Chicago, IL, USA). The statistical analysis was performed using a Student's *t*-test (for 2 groups). Statistical significant differences were considered with specific groups (**$p<0.01$ and *$p<0.05$).

Results and Discussion

Preparation, Characterization and Morphology of BA-NS

The anti-solvent method was used to produce nano-sized particles from the organic solution by dint of controlled precipitation, respectively.[28] In the present process, a solvent screening revealed methanol was a good solvent of BA. Stabilizers widely used in literatures include poloxamers, polysorbates, lecithins and povidones.[29] Finally, SDS and PVP K29-32 were identified as stabilizers to prepare BA-NS.

It is well known that PS and Zeta potential are significant characteristics for the evaluation of the stability in nanosystem and suggest the physiochemical behaviors of the formulation, involving dissolution velocity, saturation solubility and physical stability. Zeta potential indicates the stability of the nanoparticles to

be stably dispersed in suspension.[30] The PS and the Zeta potential of the BA-NS were 129.7±12.2 nm and −28.1 ±4.5 mV, respectively, in Figure 3A and B, and the PDI was 0.232±0.013. The photograph of BA-NS showed clear and consistent opalescence in Figure 3C, which further confirmed that the good uniform distribution of BA-NS to improve the nanosuspension physical stability.

The TEM micrograph of the BA-NS is shown in Figure 3D, which revealed that the BA nanoparticles were spherical or near-spherical. The SEM image revealed micro-sized particles of BA in Figure 4A and B, nanosized particles of BA-NS after freeze-drying in Figure 4C and D. The morphological assays showed that the freeze-dried BA nanoparticles were generally smaller in size, more irregular in shape and spherically smoother compared with the BA powder.

Thermal Analysis by DSC

As shown in Figure 5A, thermal analysis of BA powder, physical mixture and freeze-dried BA-NS were performed by DSC. The BA powder exhibited a single sharp melt process, with an onset temperature of 313.62°C to 321.32° C and a sharp endothermic peak of 319.99°C. In contrast, this peak disappeared completely in the thermal profile of freeze-dried BA-NS, suggesting that there was no crystalline in the BA-NS. The endothermic peak of BA in the physical mixture was weakened compared to pure BA (around 200°C), which indicated no interaction between the two components. Appearance of the same peaks between the physical mixture and BA-NS may be due to the melting peaks of excipients. These results indicated that the BA nanoparticles transferred from crystal state into amorphous state during the preparation of nanosuspension, which was also supported by the X-ray analysis results.

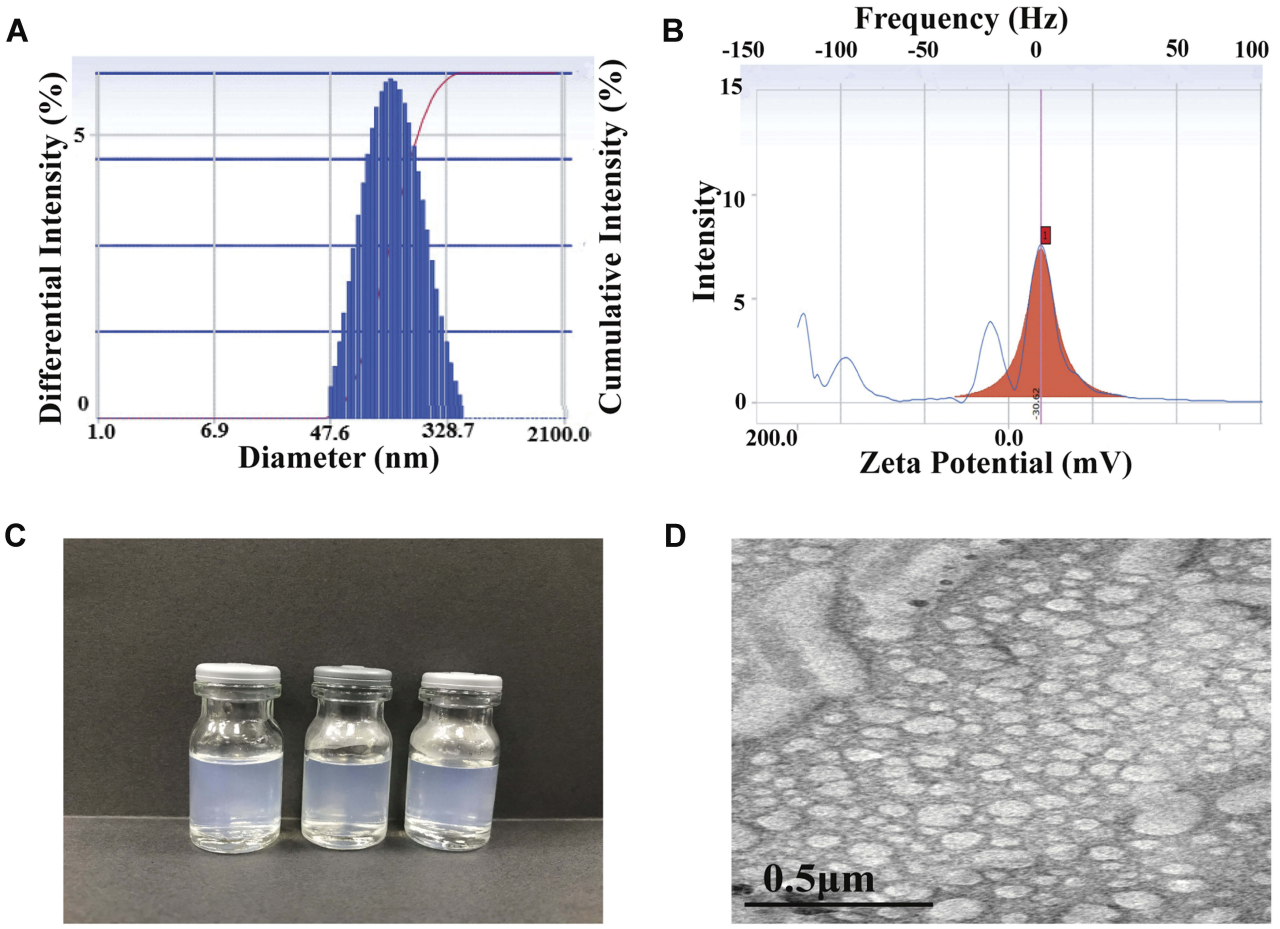

Figure 3 Characterization and TEM morphology of BA-NS. (**A**) The size distribution of BA-NS; (**B**) The Zeta potential of BA-NS; (**C**) Appearance of BA-NS and (**D**) TEM photograph of BA-NS in 8000×.

Abbreviations: BA-NS, betulinic acid nanosuspension; TEM, transmission electron microscope.

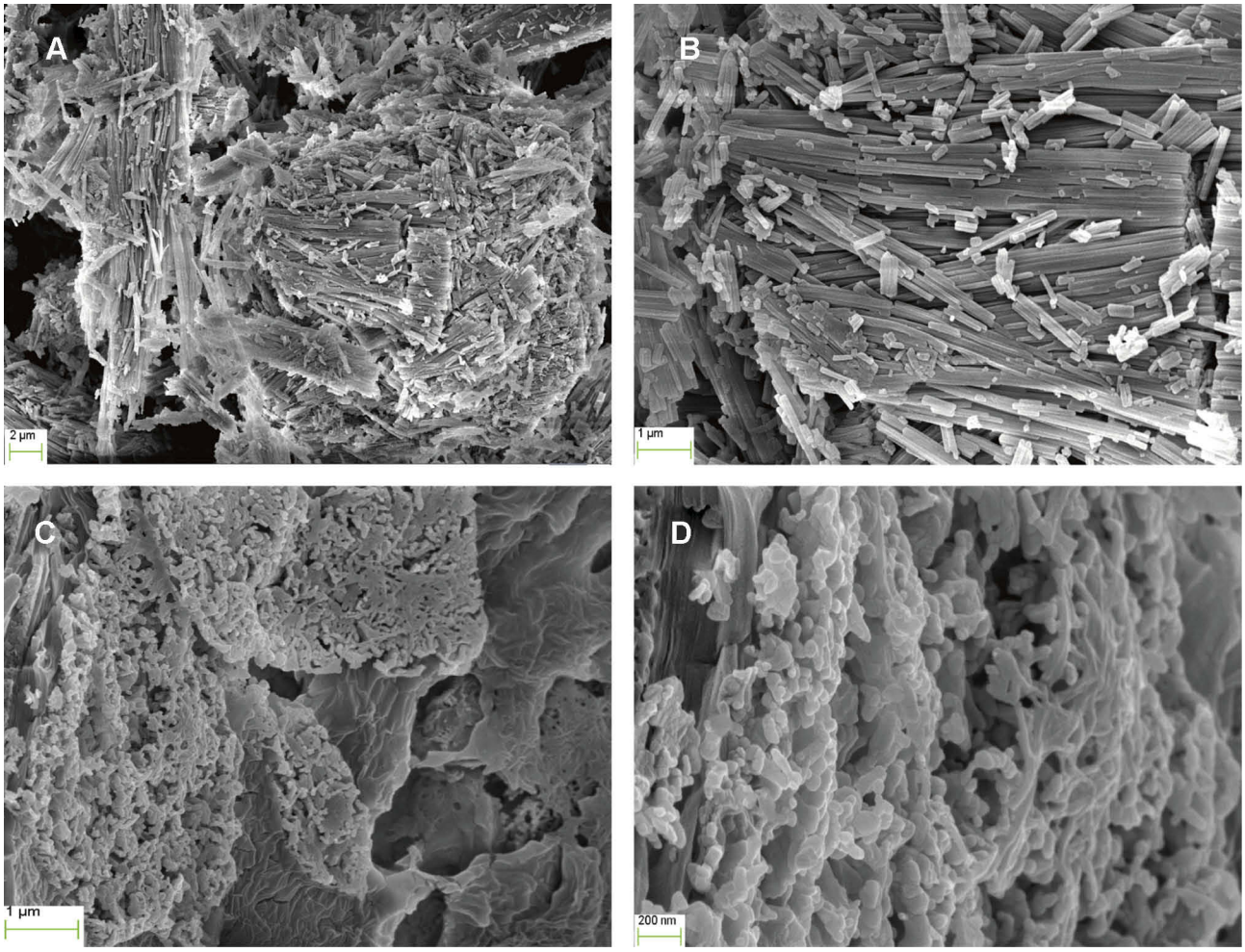

Figure 4 SEM photographs of BA in 3000×(**A**), BA in 10,000×(**B**), BA-NS in 10,000 ×(**C**) and BA-NS in 40,000 ×(**D**).
Abbreviations: SEM, scanning electron microscope; BA, betulinic acid; BA-NS, betulinic acid nanosuspension.

XRPD

X-ray diffraction study was performed to further confirm the crystalline form of BA and amorphous state of BA-NS. Figure 5B shows the XRPD of BA, physical mixture and lyophilized BA-NS. The diffraction patterns showed BA characteristic high-energy diffraction peaks at 8.37°, 13.04° and 14.35°, which demonstrated that free BA has a high degree of crystallization. In comparison, BA-NS showed peaks at 4.40° and 6.57°, but some characteristic peaks of BA were absent, which may be due to BA existed in an amorphous state in the nanoparticles. Meanwhile, in the physical mixture, the diffraction patterns of stabilizers agreed with those of the BA.

FTIR

FTIR was used to assess the interaction between BA and the excipients. The FTIR spectra of BA, their physical mixture and the BA-NS are shown in Figure 5C. In the spectrum of BA, we could conclude that the stretching vibration of C=C was at 1641.97 cm^{-1}, the peaks at 1687.74 cm^{-1} were resulting from the stretching vibration of C=O, the absorption band was detected at 3443.04 cm^{-1} due to the O-H stretching vibration. These absorption peaks all appeared and had almost the equivalent value as the curve of the nanosuspension and physical mixture, which demonstrated that the chemical structure of the drug was not changed after the precipitation process.

Solubility Analysis

According to the previous literature, we could learn about that the solubility of BA in water is 0.02 µg/mL.[31] The data showed that the water-solubility of BA-NS (15.65 ±0.76 µg/mL) was 782.5 times higher than that of BA. The above results indicated that the combination of stabilizers and BA to form nanosuspension significantly enhanced the water-solubility of BA. The decrease in the

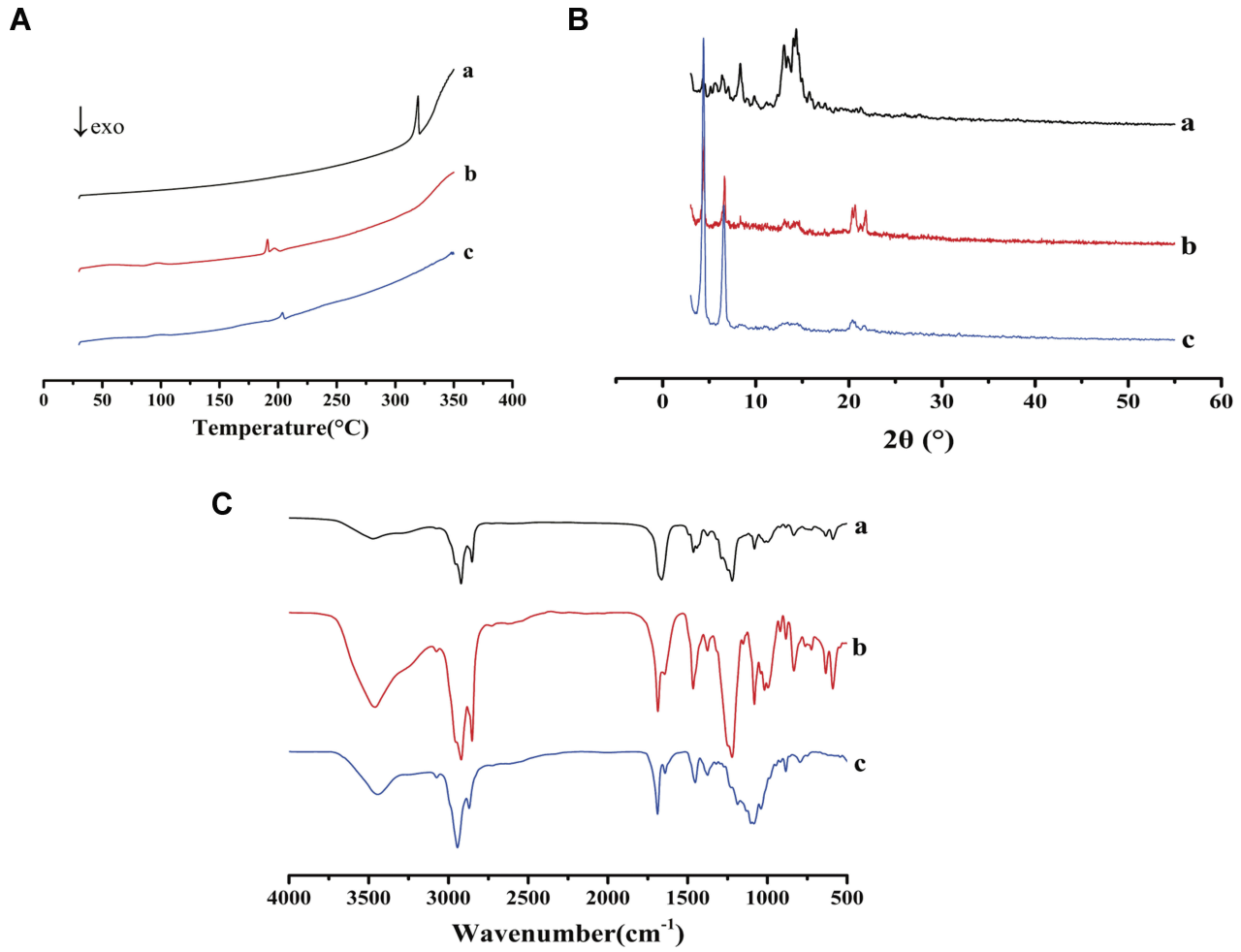

Figure 5 Characterization of BA, physical mixture and BA-NS. (**A**) DSC curves (**B**) XRD patterns (**C**) FTIR spectra.
Notes: BA (a), the physical mixture (b) and the freeze-dried powder of BA-NS (c); Results are expressed as mean ± SD (n=3).
Abbreviations: DSC, differential scanning calorimetry; BA, betulinic acid; BA-NS, betulinic acid nanosuspension; XRD, X-ray diffractometry; FTIR, Fourier transform infrared spectroscopy.

size of the nanoparticles significantly enlarged the contact area with the solvent, and good stabilizers allowed the drug particles to be uniformly dispersed in the deionized water, preventing particle aggregation and improving drug stability.[32] Therefore, nanoscale technology is a suitable method for increasing solubility of BA where solubility is the committed step in systemic absorption.[33]

Dissolution Test

The results of the dissolution rate in PBS (pH 1.2, 4.8 and 7.4) are shown in Figure 6A–C. We concluded that the dissolution rate of BA from nanosuspension at pH 1.2 (Figure 6A) was substantially lower than that at pH 4.8 and 7.4 (Figure 6B and C). There was only 25% of the BA nanoparticles dissolved in the first 10 min at pH 1.2, as opposed to more than 40% and 62% of that at PH 4.8 and 7.4, respectively. The release rates of BA from the nanosuspension were limited to 44%, 60% and 93% in PBS after 60 mins at pH 1.2, 4.8 and 7.4, respectively, suggesting the BA release profile is pH-dependent. BA is known as weak acid (pKa=5.5), as the pH increased, the more BA will be released.[34] Similarly, it was very clear that more BA from nanosuspension being released compared to the coarse BA and physical mixture in various dissolution media. According to the Noyes–Whitney equation, the decrease in particle size accompanied by an enlargement in the surface area results in an increase in dissolution rate.[35] A slight increase in the dissolution rate of the physical mixture may be attributed to the solubilization of excipients.

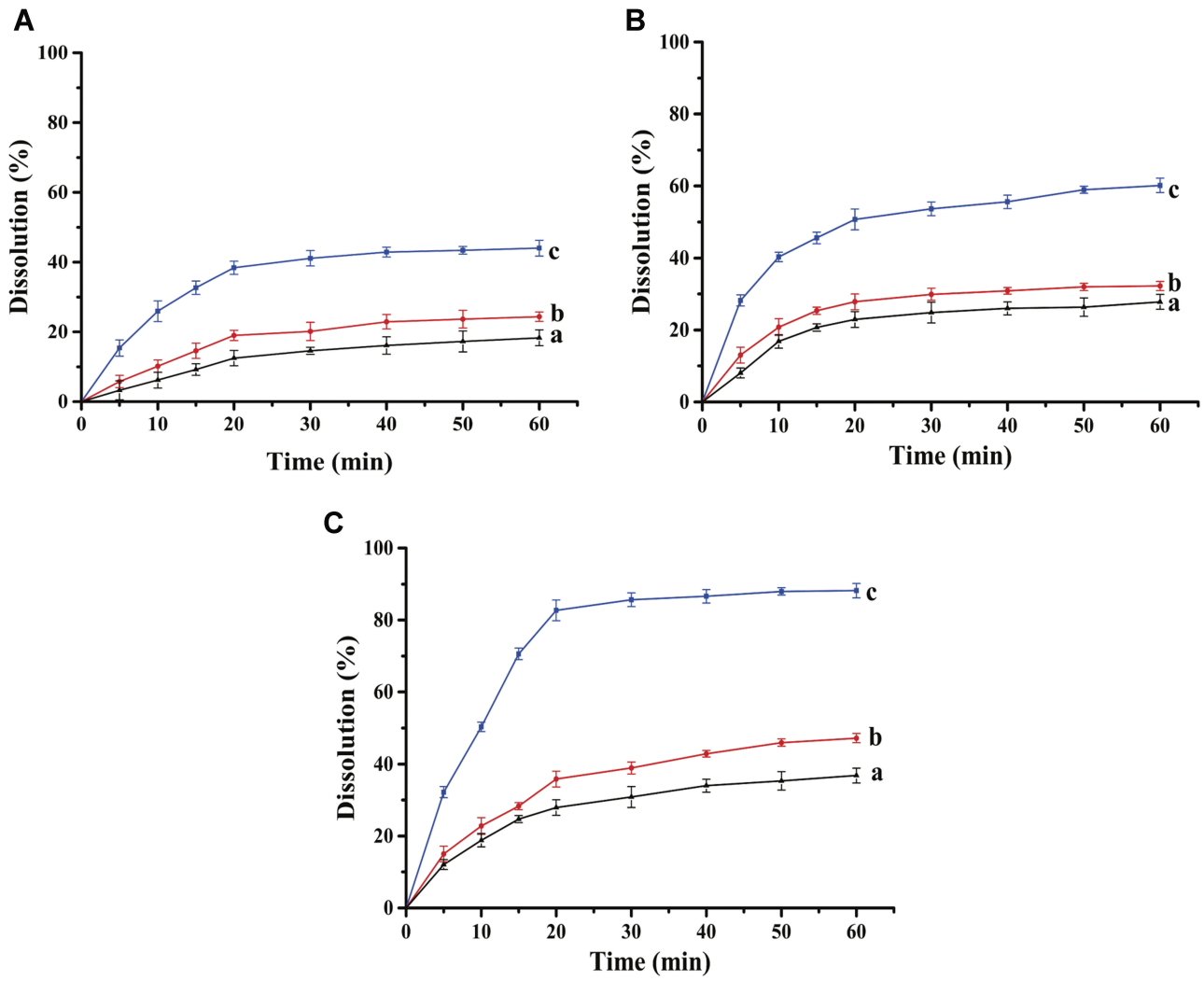

Figure 6 The dissolution studies in PBS at PH1.2 (**A**), PH4.8 (**B**) and PH7.4(**C**).
Notes: BA (a), the physical mixture (b) and the freeze-dried powder of BA-NS (c); Results are expressed as mean ± SD (n=3).
Abbreviations: PBS, phosphate buffer; BA, betulinic acid; BA-NS, betulinic acid nanosuspension.

The Optimization of BA-NS Prescription by BBD

BBD is used to assess the impact of operating parameters on the process and find the appropriate model to optimize the formulation.[36] The relationships between input factors and responses are presented by the following equation:

$$Y_1 = 243.60 - 147.74X_1 - 10.31X_2 + 109.30X_3 + 60.57X_1X_2 - 150.65X_1X_3 + 13.85X_2X_3 + 147.51{X_1}^2 + 157.26{X_2}^2 - 63.71{X_3}^2$$

$$Y_2 = 0.16 - 0.041X_1 - 0.024X_2 + 0.096X_3 + 0.088X_1X_2 - 0.067X_1X_3 - 0.026X_2X_3 + 0.061{X_1}^2 + 0.040{X_2}^2 + 0.048{X_3}^2$$

It could be seen from the correlation coefficients of the above two fitting equations that the goodness of fit index in design models was fairly good. Therefore, the optimum prescription of the BA-NS can be analyzed and predicted. The model terms with $p<0.01$ and $0.01<p<0.05$ indicated highly significant and significant, respectively. Analysis of variance in Tables 3 and 4 showed that X_1, X_3, X_1X_3, ${X_1}^2$ and ${X_2}^2$ were extremely significant in Model Y_1, while other items were insignificant; X_3 and X_1X_2 in Model Y_2 were remarkably significant compared to other groups, ${X_1}^2$ was relatively significant, but likewise other items were insignificant.

The p-values of the optimal model in this study Y_1 and Y_2 used were all less than 0.05, which indicated the model

Table 3 ANOVA of Measured Responses for Y_1

Source	Sum of Squares	DF	Mean Square	F-value	P-value	Significance
Model	593,100	9	65,904.00	12.64	0.0015	**
X_1	174,600	1	174,600	33.49	0.0007	**
X_2	850.78	1	850.78	0.16	0.6983	
X_3	95,571.92	1	95,571.92	18.33	0.0036	**
X_1X_2	14,677.32	1	14,677.32	2.82	0.1373	
X_1X_3	90,781.69	1	90,781.69	17.41	0.0042	**
X_2X_3	767.29	1	767.29	0.15	0.7126	
X_1^2	91,620.79	1	91,620.79	17.57	0.0042	**
X_2^2	104,100	1	104,100	19.97	0.0029	**
X_3^2	17,091.72	1	17,091.72	3.28	0.1131	
Residual	36,492.84	7	5213.26	–	–	
Lack of fit	17,539.54	3	5846.51	1.23	0.4072	
Pure error	18,953.30	4	4738.32	–	–	
R^2	R^2=0.9420		R^2adj=0.8675			

Note: **extremely significant.
Abbreviations: ANOVA, analysis of variance; DF, degree of freedom.

Table 4 ANOVA of Measured Responses for Y_2

Source	Sum of Squares	DF	Mean Square	F-value	P-value	Significance
Model	0.180	9	0.020	8.13	0.0057	*
X_1	0.013	1	0.013	5.41	0.0529	
X_2	0.005	1	0.005	1.97	0.2035	
X_3	0.073	1	0.073	29.97	0.0009	**
X_1X_2	0.031	1	0.031	12.76	0.0091	*
X_1X_3	0.018	1	0.018	7.36	0.0301	
X_2X_3	0.003	1	0.003	1.13	0.3232	
X_1^2	0.016	1	0.016	6.39	0.0394	*
X_2^2	0.007	1	0.007	2.71	0.1440	
X_3^2	0.010	1	0.010	4.03	0.0846	
Residual	0.017	7	0.002	–	–	
Lack of fit	0.002	3	0.001	0.20	0.8883	
Pure error	0.015	4	0.004	–	–	
R^2	R^2=0.9127		R^2adj=0.8005			

Notes: *significant. **Extremely significant.
Abbreviations: ANOVA, analysis of variance; DF, degree of freedom.

had significant difference, the values of lack of fit were insignificant (Y_1: P=0.4072>0.05, Y_2: P=0.8883>0.05), which demonstrated that the model had statistical significance; The correlation coefficient (Y_1: R^2_{adj}=0.8675 and Y_2: R^2_{adj}=0.8001) indicated that the model could explain the changes of the response value in 86.75% and 80.01%, respectively, so the fitting degree of the model was satisfactory.

According to the average PS and PDI, combined with the effect surface graphs, the optimal formulation was predicted to be 0.928 mg/mL, PVP concentration was 1.13 mg/mL, and SDS concentration was 2.12 mg/mL. Given the actual operating conditions and to improve the precision of the measured results, the calculated drug, PVP and SDS concentration were set as 1.0, 1.0 and 2.0 mg/mL, respectively.

The relationship between the independent variables and the dependent variables was further represented by a 3D graph in Figure 7.[37] Figure 7 illustrated the interactive effects of various independent variables on PS and PDI. So we could clearly see that the concentration of SDS (X_3) impacted the PS and PDI most significantly.

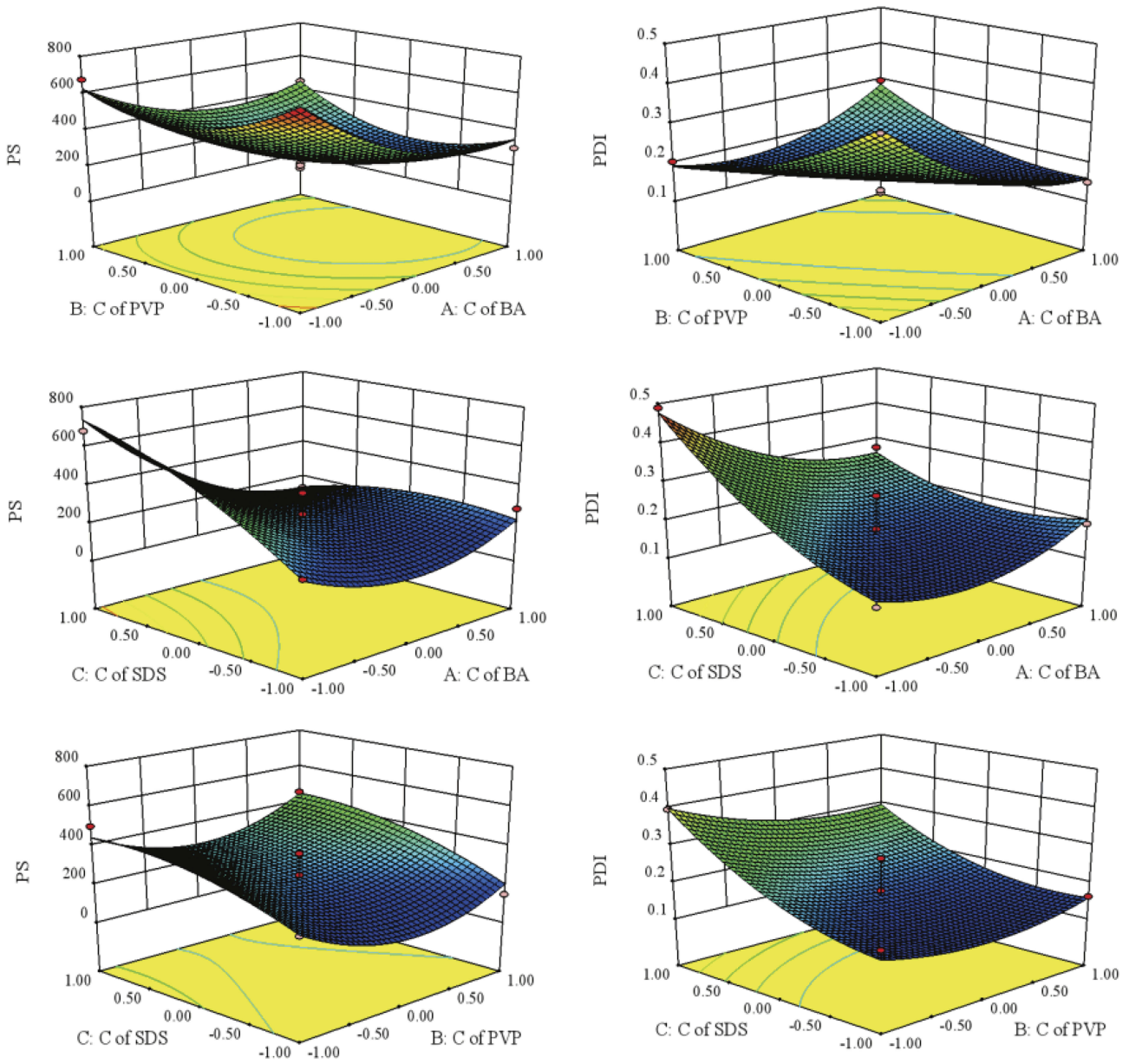

Figure 7 3D response surface plots for the PS and PDI.
Abbreviations: BA, betulinic acid; PVP, polyvinylpyrrolidone; SDS, sodium dodecyl sulfate; PS, size of particle; PDI, polydispersity index.

Physical Stability

The change in the size of the particles and variations in PDI values over time are shown in Table 5. The results indicated that the PS and PDI had no significant change and uniformed in appearance during storage.

Cytotoxicity Studies

HeLa, A549 and HepG2 were used to examine cytotoxicity under different concentrations of BA-S or BA-NS, and the inhibition ratio was evaluated by MTT assay. The theory of the MTT assay is that an increase or decrease in viable cells linearly related to mitochondrial activity which is reflected by the exchange of the tetrazolium salt into dissolved

Table 5 The Stability Investigation Results of BA-NS

Storage Time (d)	PS (nm)	PDI	Appearance
0	129.7 ±12.2	0.231 ±0.013	Clear, uniform and opalescence
30	151.3 ±10.8	0.252 ±0.025	Clear, uniform and opalescence

Notes: The data are mean ± SD of triplicate experiments (n=3).
Abbreviations: BA-NS, betulinic acid nanosuspension; PS, particle size; PDI, polydispersity index.

formazan crystals.[38] As shown in Figure 8A, the results showed that BA-NS inhibited HeLa cell growth in a dose-dependent manner. Furthermore, a significant decrease in the number of living cells was found when the cells were exposed to 60 μM. While there had no obvious increase in inhibition rate was observed in BA-S invaded cells, which may attribute to BA powders were not fully dissolved in suspension and thus were less bioavailable to HeLa cells. The IC_{50} (48 h) values of BA-S and BA-NS were >100 μM and 61.62±0.72 μM, respectively.

Figure 8B and C indicated that the cytotoxicity was also positively dose-correlated when BA-NS was exposed to A549 and HepG2 cells with IC_{50} (48 h) of 47.63±0.46 μM and 56.30±0.07 μM, respectively. Simultaneously, the results of the two blank-NS invaded cell lines were similar to those of HeLa cells, that is, no significant toxicity was found, implying the inhibitory effect of the excipients on cells was negligible. The results suggested that the IC_{50} value of BA-NS on tumor cells was apparently lower compared with BA-S after the same incubation time. BA-NS has superior cytotoxicity on A549, which was consistent with previous work.[39]

Conclusion

In summary, in order to improve its solubility, we have prepared the optimum BA-NS for using in new drug delivery system by an appropriate antisolvent method, and the optimal formulation was obtained by BBD. The PS and particle morphology of BA-NS (<200 nm) illustrated that the formulation can effectively reduce the size of BA powder particles and the distribution was uniform and stable. FTIR and DSC indicated that the drug was not affected by excipients and experimental manipulations. The dissolution rates showed that the BA-NS release profile was pH-dependent. The BA-NS was significantly more cytotoxic to HeLa, A549 and HepG2 cell lines compared to the native BA. However, it is worth noting that the distribution of BA-NS into the human body and how to inhibit the growth of tumor cells need to be

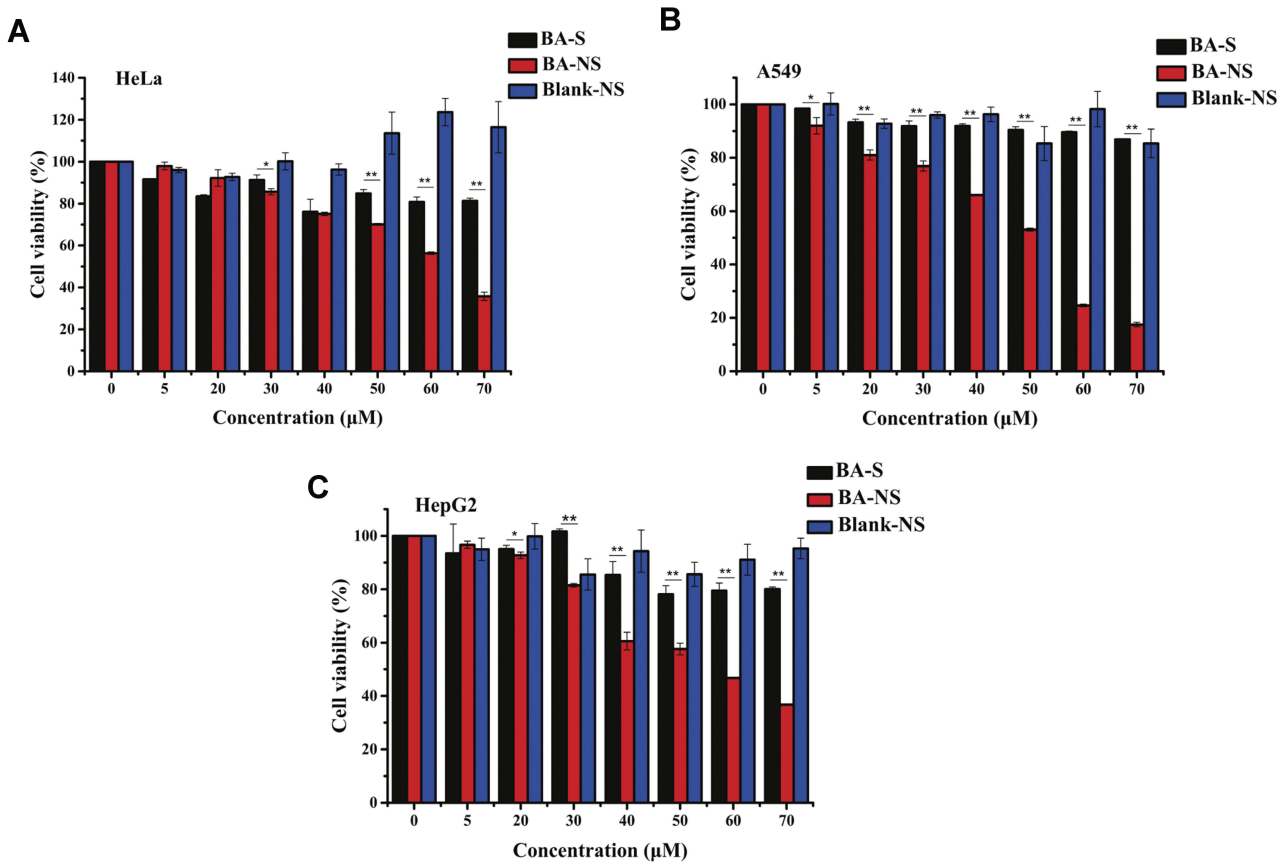

Figure 8 In vitro cytotoxicity study of (**A**) HeLa, (**B**) A549, and (**C**) HepG2 exposed to BA-S, BA-NS and blank-NS, respectively.
Notes: The data are mean ± SD of triplicate experiments (n=3). *significant; **extremely significant.
Abbreviations: BA-S, betulinic acid suspension; BA-NS, betulinic acid nanosuspension; Blank-NS, blank nanosuspension; ns, not significant.

studied, which lays a theoretical foundation for further modification.

Acknowledgment

This work was financially supported by the National Nature Science Foundation of China (number 81403111); the R&D Team for Formulation Innovation (Grant No 2015CXQX150); Guangzhou Science and Technology Plan Project (number 201904010112); and the "Yang Fan Plan" team project of Guangdong Province (No. 2017Y T05S137).

Disclosure

The authors report no conflicts of interest in this work.

References

1. Yogeeswari P, Sriram D. Betulinic acid and its derivatives: a review on their biological properties. *Curr Med Chem*. 2005;12(6):657–666. doi:10.2174/0929867053202214
2. Eiznhamer DA, Xu Z. Betulinic acid: a promising anticancer candidate. *IDrugs*. 2004;7(4):359.
3. Kessler JH, Mullauer FB, de Roo GM, et al. Broad in vitro efficacy of plant-derived betulinic acid against cell lines derived from the most prevalent human cancer types. *Cancer Lett*. 2007;251 (1):132–145. doi:10.1016/j.canlet.2006.11.003
4. Oliveira Costa JF, Barbosa-Filho JM, de Azevedo Maia GL, et al. Potent anti-inflammatory activity of betulinic acid treatment in a model of lethal endotoxemia. *Int Immunopharmacol*. 2014;23 (2):469–474. doi:10.1016/j.intimp.2014.09.021
5. Holz-smith SL, Sun IC, Jin L, et al. Role of Human Immunodeficiency Virus (HIV) Type 1 envelope in the anti-HIV activity of the betulinic acid derivative IC9564. *Antimicrob Agents Ch*. 2001;1(45):60–66. doi:10.1128/AAC.45.1.60-66.2001
6. Selzer E, Pimentel E, Wacheck V, et al. Effects of betulinic acid alone and in combination with irradiation in human melanoma cells. *J Invest Dermatol*. 2000;114(5):935–940. doi:10.1046/j.1523-1747.2000.00972.x
7. Chintharlapalli S, Papineni S, Ramaiah SK, et al. Betulinic acid inhibits prostate cancer growth through inhibition of specificity protein transcription factors. *Cancer Res*. 2007;67(6):2816–2823. doi:10.1158/0008-5472.CAN-06-3735
8. Fulda S, Friesen C, Los M, et al. Betulinic acid triggers CD95 (APO-1/ Fas)- and p53-independent apoptosis via activation of caspases in neuroectodermal tumors. *Cancer Res*. 1997;57(21):4956–4964.
9. Zuco V, Supino R, Righetti SC, et al. Selective cytotoxicity of betulinic acid on tumor cell lines, but not on normal cells. *Cancer Lett*. 2002;175(1):17–25. doi:10.1016/S0304-3835(01)00718-2
10. Fulda S, Kroemer G. Targeting mitochondrial apoptosis by betulinic acid in human cancers. *Drug Discov Today*. 2009;14(17–18): 885–890. doi:10.1016/j.drudis.2009.05.015
11. Cheng Z, Chen AF, Wu F, et al. 8,8-Dimethyldihydroberberine with improved bioavailability and oral efficacy on obese and diabetic mouse models. *Bioorg Med Chem*. 2010;18(16):5915–5924. doi:10.1016/j.bmc.2010.06.085
12. Saneja A, Kumar R, Singh A, et al. Development and evaluation of long-circulating nanoparticles loaded with betulinic acid for improved anti-tumor efficacy. *Int J Pharm*. 2017;531(1):153–166. doi:10.1016/j.ijpharm.2017.08.076
13. Guo BH, Xu DQ, Liu XH, et al. Enzymatic synthesis and in vitro evaluation of folate-functionalized liposomes. *Drug Des Devel Ther*. 2017;11:1839–1847. doi:10.2147/DDDT.S132841
14. Kumar P, Singh AK, Raj V, et al. Poly(lactic-co-glycolic acid)-loaded nanoparticles of betulinic acid for improved treatment of hepatic cancer: characterization, in vitro and in vivo evaluations. *Int J Nanomedicine*. 2018;13:975–990. doi:10.2147/IJN.S157391
15. Mosharraf M, Nyström C. The effect of particle size and shape on the surface specific dissolution rate of microsized practically insoluble drugs. *Int J Pharmaceut*. 1995;122(1):35–47. doi:10.1016/0378-5173(95)00033-F
16. Lou HY, Gao L, Wei XB, et al. Oridonin nanosuspension enhances anti-tumor efficacy in SMMC-7721 cells and H22 tumor bearing mice. *Colloids Surf B*. 2011;87(2):319–325. doi:10.1016/j.colsurfb.2011.05.037
17. Kocbek P, Baumgartner S, Kristl J. Preparation and evaluation of nanosuspensions for enhancing the dissolution of poorly soluble drugs. *Int J Pharmaceut*. 2006;312(1):179–186. doi:10.1016/j.ijpharm.2006.01.008
18. Wang YC, Ma YY, Zheng Y, et al. In vitro and in vivo anticancer activity of a novel puerarin nanosuspension against colon cancer, with high efficacy and low toxicity. *Int J Pharmaceut*. 2013;441 (1–2):728–735. doi:10.1016/j.ijpharm.2012.10.021
19. Shen S, Mamat M, Zhang SC. Synthesis of CaO_2 nanocrystals and their spherical aggregates with uniform sizes for use as a biodegradable bacteriostatic agent. *Small*. 2019;15(36):1–7. doi:10.1002/smll.v15.36
20. Verma S, Gokhale R, Burgess DJ. A comparative study of top-down and bottom-up approaches for the preparation of micro/nanosuspensions. *Int J Pharmaceut*. 2009;380(1–2):216–222. doi:10.1016/j.ijpharm.2009.07.005
21. Chavhan SS, Petkar KC, Sawant KK. Nanosuspensions in drug delivery: recent advances, patent scenarios, and commercialization aspects. *Crit Rev Ther Drug*. 2011;28(5):447. doi:10.1615/CritRevTherDrugCarrierSyst.v28.i5
22. Chan HK, Chi Lip Kwok P. Production methods for nanodrug particles using the bottom-up approach. *Adv Drug Deliver Rev*. 2011;63 (6):406–416. doi:10.1016/j.addr.2011.03.011
23. Zhang HX, Wang JX, Zhang ZB, et al. Micronization of atorvastatin calcium by antisolvent precipitation process. *Int J Pharmaceut*. 2009;374(1–2):106–113. doi:10.1016/j.ijpharm.2009.02.015
24. Gajera BY, Shah DA, Dave RH. Development of an amorphous nanosuspension by sonoprecipitation-formulation and process optimization using design of experiment methodology. *Int J Pharmaceut*. 2019;559:348–359. doi:10.1016/j.ijpharm.2019.01.054
25. Jojo GM, Kuppusamy G. Formulation and optimization of intranasal nanolipid carriers of pioglitazone for the repurposing in Alzheimer's disease using Box-Behnken design. *Drug Dev Ind Pharm*. 2019;45 (7):1061–1072. doi:10.1080/03639045.2019.1593439
26. Ren LL, Wang JJ, Chen GG. Preparation, optimization of the inclusion complex of glaucocalyxin A with sulfobutylether-β-cyclodextrin and antitumor study. *Drug Deliv*. 2019;26(1):309–317. doi:10.1080/10717544.2019.1568623
27. Ferrari M, Fornasiero MC, Isetta AM. MTT colorimetric assay for testing macrophage cytotoxic activity in vitro. *J Immunol Methods*. 1990;131(2):165. doi:10.1016/0022-1759(90)90187-Z
28. Kathpalia H, Juvekar S, Shidhaye S. Design and in vitro evaluation of atovaquone nanosuspension prepared by pH based and anti-solvent based precipitation method. *Colloid Interface Sci Commun*. 2019;29:26–32. doi:10.1016/j.colcom.2019.01.002
29. Cornelia MK, Rainer HM. Drug nanocrystals of poorly soluble drugs produced by high pressure homogenisation. *Eur J Pharm Biopharm*. 2006;62(1):3–16. doi:10.1016/j.ejpb.2005.05.009
30. Arunkumar N, Deecaraman M, Rani C. Nanosuspension technology and its applications in drug delivery. *Asian J Pharm*. 2009;3(3):168. doi:10.4103/0973-8398.56293
31. Jäger S, Winkler K, Pfüller U, et al. Solubility studies of oleanolic acid and betulinic acid in aqueous solutions and plant extracts of viscum L. *Planta Med*. 2007;73(2):157–162. doi:10.1055/s-2007-967106

32. Gao Y, Li ZG, Sun M, et al. Preparation and characterization of intravenously injectable curcumin nanosuspension. *Drug Deliv*. 2011;18(2):131–142. doi:10.3109/10717544.2010.520353
33. Sharma P, Garg S. Pure drug and polymer based nanotechnologies for the improved solubility, stability, bioavailability and targeting of anti-HIV drugs. *Adv Drug Deliver Rev*. 2010;62(4–5):491–502. doi:10.1016/j.addr.2009.11.019
34. Du H, Chen XQ. CD-MEKC method to analyze triterpene acids in traditional Chinese medicines. *J Braz Chem Soc*. 2009;20 (7):1268–1274. doi:10.1590/S0103-50532009000700011
35. Hintz RJ, Johnson KC. The effect of particle size distribution on dissolution rate and oral absorption. *Int J Pharm*. 1989;51:9–17. doi:10.1016/0378-5173(89)90069-0
36. Mohammad A, Abdulhameed AS, Jawad AH. Box-Behnken design to optimize the synthesis of new crosslinked chitosan-glyoxal/TiO2 nano-composite: methyl orange adsorption and mechanism studies. *Int J Biol Macromol*. 2019;129:98–109. doi:10.1016/j.ijbiomac.2019.02.025
37. Kumar M, Dahuja A, Sachdev A, et al. Valorisation of black carrot pomace: microwave assisted extraction of bioactive phytoceuticals and antioxidant activity using Box-Behnken design. *J Food Sci Technol*. 2019;56(2):995–1007. doi:10.1007/s13197-018-03566-9
38. Meerloo JV, Kaspers GJL. Cell sensitivity assays: the MTT assay. *Methods Mol Biol*. 2011;(731):237–245.
39. Hong EH, Song JH, Kang KB, et al. Anti-influenza activity of betulinic acid from *Zizyphus jujuba* on influenza A/PR/8 virus. *Biomol Ther*. 2015;23(4):345–349. doi:10.4062/biomolther.2015.019